

Monte Carlo rejection as a tool for measuring the energy landscape scaling of simple fluids

Gerardo G. Naumis

Instituto de Física, Universidad Nacional Autónoma de México (UNAM), Apartado Postal 20-364, 01000, México, Distrito Federal, Mexico

(Received 27 January 2005; published 31 May 2005)

A simple modification of the Monte Carlo algorithm is proposed to explore the topography and the scaling of the energy landscape. We apply this idea to a simple hard-core fluid. The results for different packing fractions show a power law scaling of the landscape boundary, with a characteristic scale that separates the values of the scaling exponents. Finally, it is shown how the topology determines the freezing point of the system due to the increasing importance and complexity of the boundary.

DOI: 10.1103/PhysRevE.71.056132

PACS number(s): 64.70.Pf, 61.20.-p, 68.18.Jk

I. INTRODUCTION

A liquid cooled to temperatures near its freezing point can be conduced to a glassy state or to a crystal according to the speed of cooling [1]. When the speed is high enough, the supercooled liquid undergoes a glass transition to a state that is disordered, while a phase transition of the type fluid crystal is obtained if the system is kept in thermodynamical equilibrium at all steps of the cooling path [2]. The understanding of the many different aspects of glass transition still remains as one of the most important problems in physics [3], as for example, the explanation of the nonexponential relaxation of fluctuations [4] or why not all materials form glasses [5]. Another very interesting property of glasses, related with the glass forming tendency [6], is the behavior of the viscosity, which is usually referred as fragility. Different approaches have been used to understand glass transition: models like the Gibbs-DiMarzio [7], theories like the mode coupling, stochastic agglomeration [8–10] or the use of computer simulations [7]. Another useful approach is the rigidity theory of Phillips [11] and Thorpe [12], which relates the ratio between available degrees of freedom and the number of constraints [13]. In previous works, we showed that even for simple systems like hard disks [14] and colloids [15], it seems that rigidity plays an important role even for the case of a simple phase transition, since it is clear that in order to form a solid, the system must develop certain rigidity. Some works on the relaxation properties of colloids, seem to confirm these ideas [16].

Parallel to all of these approaches, there is another formalism that has been very useful to visualize and understand what happens during a glass or usual phase transition. This formalism is the energy landscape approach [17,18], which many years ago was very successful in the field of spin glasses [19]. The main idea behind this approach, is that the landscape is a surface generated by the potential energy of the system as a function of the molecular positions [2]. For a system with N molecules, the landscape is determined by the potential energy function, $\Phi(\mathbf{r}_1, \dots, \mathbf{r}_N)$, where \mathbf{r}_i comprise all relevant coordinates, like position and orientation. Since the kinetic energy (K) is a positive defined quantity, the system evolves in such a way that $K = E - \Phi(\mathbf{r}_1, \dots, \mathbf{r}_N) \geq 0$, where E is the total energy. The topography of the landscape

energy surface determines the possible evolution of the system, and the contact with thermodynamics is made by using statistical mechanics [2]. The great advantage of the landscape formalism is that it can be used even without thermodynamical equilibrium. In such a case, ergodicity is broken and the entropy is not a maximum anymore, as postulated in the usual equilibrium statistical mechanics. The main question to be answered for this case, is to figure out the fraction of allowed volume in phase space that is visited by the system.

The usual picture of a phase or glass transition in such a language, is that at high temperatures the system does not feel the topology of $\Phi(\mathbf{r}_1, \dots, \mathbf{r}_N)$ because the kinetic energy contribution dominates. As the temperature is lowered, the system is unable to surmount the highest energy barriers and therefore is forced to sample deep minima. For a slow cooling is slow, the system has time to find a path to the most stable state, an ordered crystal. It will be trapped in a metastable state, the glass [17,18], if the cooling speed is high enough. Many works that relates the statistics of an energy landscape with the thermodynamical properties of the system have been made [2,20–23], and even some phenomenological relations between rigidity and the energy landscape have been obtained [24]. For a Lennard-Jones fluid, it has been determined that the network of minima is a static scale-free network [25].

However, up to now there are some important questions that remain, for example, what is the topography of the landscape for a fragile liquid or how to obtain the viscosity [18], diffusion [26] and rigidity from the landscape [24]. Also, although is widely believed that the landscape is fundamental to understand many features of a liquid, still is not completely clear how to use the landscape topology to predict a phase transition [27]. Another interesting question is what is the nature of the texture of the landscape? In other words, is the topography a fractal? What's the fractal dimension of the landscape? Although some of these questions seem to have an academic interest only, is clear that the relaxation properties of a very complex fractal landscape are different from a smooth landscape [28], where the system can easily explore the phase space. In this article, we will explore some of these questions by looking at the scaling of the landscape.

The layout of this work is the following: in Sec. II we discuss how to use a modified Monte Carlo method to study

the scaling. In Sec. III we apply the method to a simple fluid of hard disks. Finally, in Sec. IV we give the conclusions.

II. MONTE CARLO REJECTION AND SCALING OF THE LANDSCAPE

In this section we will develop a method to relate the Monte Carlo rejection ratio and the scaling of the landscape. Before going into the details, it would be useful to explain some others approaches to obtain information about the landscape topology. To simplify ideas, in this article we will use as a model system, N hard disks or spheres of diameter σ in a given area (S) or volume (V). In such hard-core particle system, the energy landscape is formed by walls of infinite height that divide the allowed and forbidden regions of the configurational phase space. If \mathbf{r}_i is the position of a disk or sphere i , the allowed region of the landscape is the set of points where

$$\|\mathbf{r}_i - \mathbf{r}_j\| \geq \sigma, \quad (1)$$

for all possible pairs i and j . The number of such pairs (R_{NH}) is the number of combinations of N objects taken in pairs: $C_2^N = N(N-1)/2$. Each of these C_2^N equations is a non-holonomic restriction to the system. A state \mathbf{P} in phase space is in the boundary of the landscape, if at least one of the inequalities (1) is transformed into an holonomic restriction,

$$\|\mathbf{r}_l - \mathbf{r}_m\| = \sigma, \quad (2)$$

for a pair of disks that we denote by l and m . For each equation of this type that is satisfied, two disks are in contact. For a given packing fraction (ϕ), the number of such equations (R_H) is just

$$R_H = \frac{\langle Z(\phi) \rangle}{2} N, \quad (3)$$

where $\langle Z(\phi) \rangle$ is the average coordination per particle in a given packing. We remark that this equation allows a straightforward manner to connect the energy landscape formalism with the rigidity theory, where the most important parameter [11] is $\langle Z(\phi) \rangle$. This approach also provides a way to construct inherent structures and the boundary of the landscape just by considering a nonlinear optimization problem. To get a packing, we can define an objective function as

$$F(\mathbf{P}) = \sum_{l=1}^N \|\mathbf{r}_l\|, \quad (4)$$

with R_H constraints $\|\mathbf{r}_l - \mathbf{r}_m\| = \sigma$. This objective function is defined in such a way that the particles are packed in a tight way with respect to the origin. Surprisingly, this criteria is similar to the center of mass minimization that has been observed very recently in experiments with colloids [29,30]. In principle, this problem can be solved using nonlinear programming [31], and there is some similar work done into this line of research [32]. Here we will not follow this path. Instead, we investigate how the landscape boundary looks at different scales in the configurational part of the phase space. The most simple way to do this, consists in applying a box-

counting algorithm [33] once the boundary points are determined. In this box counting algorithm, a grid made from cubes of linear size δ is applied to the configurational phase space. Then the number of boxes that contains a boundary state are counted. The counting is repeated at different lengths δ . This ideal situation has the problem that we need to generate all the boundary states, and due to the size of the phase space, this task is almost impossible to do. A simpler approach is to take advantage of the Monte Carlo importance sampling to obtain information about the boundary.

In the Metropolis Monte Carlo method [34,35], when a system is in a microstate \mathbf{P}_0 , a movement to a new microstate \mathbf{P} is allowed if the difference in energies $\Delta E = E(\mathbf{P}) - E(\mathbf{P}_0)$ is negative [where $E(\mathbf{P})$ is the energy of the state \mathbf{P}]. If $\Delta E > 0$, a random number is compared with ΔE . In the case of hard-core systems, a rejection occurs when a new proposed configuration is not allowed by the restrictions [35], i.e., when there is an overlap between disks or spheres. When the new proposed point \mathbf{P} is rejected, one can be sure that the boundary of the landscape has been crossed, i.e., the boundary is between states \mathbf{P}_0 and \mathbf{P} . Thus, the information about the boundary can be extracted from the acceptance ratio of the Monte Carlo method, although two modifications are needed. In the usual Monte Carlo method, the trial movement distance between two states is a continuous random variable [36]. This feature is not convenient because it does not provide an approximate location for the boundary. A second fact to take into account, is that the probability of hitting the point \mathbf{P} not only depends on the size of the boundary, but also in the transient probability of the process [37] $\mathbf{P}_0 \rightarrow \mathbf{P}$. To solve these problems, let us introduce a regular grid in the configurational part of the phase space. If the simulation is performed in a box of linear length L , there are $M = (L/\delta)^{DN}$ points in the grid, where D is the dimensionality of the system. In such a grid, a random walk in phase space is performed by choosing at random a disk \mathbf{r}_i and changing one component at random to $\pm\delta$. If \mathbf{P} is written in generalized coordinates q_j , the trial movement is written as

$$(q_1, q_2, q_3, \dots, q_{DN}) \rightarrow (q_1, q_2, q_3, \dots, q_r \pm \delta, \dots, q_{DN}), \quad (5)$$

for the r coordinate chosen at random with an uniform distribution.

The introduction of a random walk is convenient because (1) the step size can be varied to look at the scaling and (2) when a movement is rejected, the state can be considered as a boundary point, since it is connected to the interior of the forbidden part of the phase space. In spite of this, the introduction of a random walk has the inconvenience of not being able to sample the phase space with equal probabilities, i.e., it is not completely ergodic and does not fulfill detailed balance. In fact, even for the usual Monte Carlo method there is some lack of ergodicity due to the existence of a finite-size underlying grid. The only difference between the simple random walk and the usual Monte Carlo method with jumps of variable size is the higher interconnectivity of the grid in the former case, which mitigates but does not solve completely the effects of the biased sampling. The main effect of this problem upon our calculations, is that the size of the boundary will be underestimated, and that some parts of the

landscape are not going to be visited. Thus the method works better before a transition, and in fact only provides a bound for the scaling exponents. Since the random walk does not fulfill detailed balance and ergodicity, one can ask if this choice is unique. In fact, the box counting algorithm can be used with other methods of sampling the phase space, as for example the hit and miss technique. However, its efficiency is usually much lower. A better way to improve upon this method, is to use other sampling algorithms that generate the boundary of the landscape in an efficient way, as for example, collision prediction [38].

Now let $p_k(\delta)$ be the probability of state k in phase space to be occupied by the system when a grid of scale δ is chosen. The random walk process can be viewed as a Markov chain [37], where the probabilities of visiting each microstate are contained in a vector. The probabilities at each step are transformed according to a stochastic matrix that contains as elements the probability of transition among states,

$$\begin{pmatrix} p'_1(\delta) \\ p'_2(\delta) \\ \dots \\ p'_M(\delta) \end{pmatrix} = \begin{pmatrix} S_{11} & S_{12} & \dots & S_{1M} \\ S_{21} & S_{22} & \dots & S_{2M-1} \\ \dots & \dots & \dots & \dots \\ S_{M1} & \dots & \dots & S_{MM} \end{pmatrix} \begin{pmatrix} p_1(\delta) \\ p_2(\delta) \\ \dots \\ p_M(\delta) \end{pmatrix},$$

where the rows of the matrix are normalized to 1, and $p'_k(\delta)$ are the probabilities after a step is made. In a hard-core system, jumps only occur between allowed grid points that are first neighbors. An element S_{rt} of this matrix is zero when one of the states r or t is in the forbidden part of the landscape. S_{rt} is also zero if r or t are not first neighbors. The only elements different from zero are $S_{rt}=1/z_r(\delta)$, if r and t are allowed neighbors, where $z_r(\delta)$ is the coordination in phase space of site t (i.e., the number of allowed first neighbors of t) for a given scale δ . Points at the boundary of the landscape are the ones where $z_r(\delta) < 2DN$ since they are connected to points inside the forbidden part of the phase space. A matrix of this type has at least one eigenvector with eigenvalue one, while the others have norms equal or less than one [9]. Thus, after successive applications of the matrix, the stable configuration is given by the eigenvalue with norm one, from where it follows that the final probabilities satisfy [9]

$$\begin{pmatrix} p_1(\delta) \\ p_2(\delta) \\ \dots \\ p_M(\delta) \end{pmatrix} = \begin{pmatrix} S_{11} & S_{12} & \dots & S_{1M} \\ S_{21} & S_{22} & \dots & S_{2M-1} \\ \dots & \dots & \dots & \dots \\ S_{M1} & \dots & \dots & S_{MM} \end{pmatrix} \begin{pmatrix} p_1(\delta) \\ p_2(\delta) \\ \dots \\ p_M(\delta) \end{pmatrix}.$$

This matrix is similar to the Hamiltonian of a binary alloy in an hypercubic lattice, where the two self-energies are very different [39] (split band regimen). It is easy to prove that the final equilibrium vector coincides with the bonding state (which corresponds with the maximal wavelength of the solution, and nearly zero phase difference between sites) of the binary alloy.

In a Monte Carlo step, the probability of having a rejection is given by the probability of jumping into a boundary point [$p_k(\delta)$], multiplied by the probability of jumping from

a state k into a state t in the forbidden region of the landscape, which is given by the elements of the stochastic matrix. Thus the probability of landing in a forbidden state t is

$$p_t(\delta) = \left(\frac{2DN - z_k(\delta)}{2DN} \right) p_k(\delta). \quad (6)$$

If $\mathcal{L}_B(\delta)$ denotes the set of all boundary points, the total probability of having rejections at a scale δ [we denote this probability by $p^R(\delta)$] is obtained by summing over all boundary states k ,

$$p^R(\delta) \equiv \sum_{k \in \mathcal{L}_B(\delta)} \left(1 - \frac{z_k(\delta)}{2DN} \right) p_k(\delta). \quad (7)$$

Now we write $z_k(\delta)$ as an average plus a fluctuation part, $z_k(\delta) = \langle z(\delta) \rangle + \Delta z_k(\delta)$, where

$$\langle z(\delta) \rangle = \frac{1}{M_B(\delta)} \sum_{k \in \mathcal{L}_B(\delta)} z_k(\delta), \quad (8)$$

and $M_B(\delta)$ is simply the number of boundary points at a scale δ . The same procedure can be made for $p_k(\delta)$, giving $p_k(\delta) = \langle p_B(\delta) \rangle + \Delta p_k(\delta)$, where $\langle p_B(\delta) \rangle$ is defined as

$$\langle p_B(\delta) \rangle = \frac{1}{M_B(\delta)} \sum_{k \in \mathcal{L}_B(\delta)} p_k(\delta). \quad (9)$$

Using these definitions, and that the sum of the fluctuations is zero, Eq. (7) is rewritten as

$$p^R(\delta) = \sum_{k \in \mathcal{L}_B(\delta)} \left(1 - \frac{\langle z(\delta) \rangle}{2DN} \right) \langle p_B(\delta) \rangle - \sum_{k \in \mathcal{L}_B(\delta)} \left(\frac{\Delta z_k(\delta) \Delta p_k(\delta)}{2DN} \right).$$

The term $\sum \Delta z_k(\delta) \Delta p_k(\delta)$ is a measure of the correlation between state and coordination fluctuations. Since the eigenvector with eigenvalue one corresponds to a bonding state in a binary alloy, using a variational procedure with a trial function or analyzing the spectral moments [39], it can be proved that $\Delta p_k(\delta) \approx \Delta z_k(\delta) / 2DN$. This term gives a correction of order

$$\frac{1}{2DN} \sum_{k \in \mathcal{L}_B(\delta)} \Delta z_k(\delta) \Delta p_k(\delta) \approx \left(\frac{\hat{\sigma}(\delta)}{2DN} \right)^2, \quad (10)$$

where $\hat{\sigma}(\delta)$ is the standard deviation of the phase space coordination distribution $z_k(\delta)$. Thus it follows that

$$M_B(\delta) \langle p_B(\delta) \rangle = \frac{p^R(\delta) + \left(\frac{\hat{\sigma}(\delta)}{2DN} \right)^2}{\left(1 - \frac{\langle z(\delta) \rangle}{2DN} \right)}. \quad (11)$$

We notice that $M_B(\delta) \langle p_B(\delta) \rangle$ is a bound for the size of the whole boundary of the landscape. For example, when the sampling is uniform, $M_B(\delta) \langle p_B(\delta) \rangle = M_B(\delta) / M(\delta)$, since $\langle p_B(\delta) \rangle = 1 / M(\delta)$. The number of grid points $M(\delta)$ scales as δ^{-DN} , and if the boundary has a scaling of the type

$M_B(\delta) \sim \delta^{-D_B N}$, then we expect a scaling of Eq. (11) as

$$\frac{M_B(\delta)}{M(\delta)} \propto (\delta/\sigma)^{D_f}, \quad (12)$$

where $D_f = (D - D_B)N$ is an effective fractal dimension due to the different scalings of the boundary and volume of the landscape. In general, states at the boundary are less visited, thus we get the following inequality:

$$M_B(\delta) \langle p_B(\delta) \rangle \leq \frac{M_B(\delta)}{M(\delta)}. \quad (13)$$

As a result, we get a bound for this scaling exponent,

$$D_f \leq \ln \left(\frac{p^R(\delta) + \left(\frac{\hat{\sigma}(\delta)}{2DN} \right)^2}{\left(1 - \frac{\langle z(\delta) \rangle}{2DN} \right)} \right) / \ln(\delta/\sigma). \quad (14)$$

The evaluation of this bound can be easily implemented inside a Monte Carlo simulation; it only requires the rejection probability $p^R(\delta)$, the average coordination $\langle z(\delta) \rangle$, and the fluctuations $\hat{\sigma}(\delta)$. To do this, first we divide the phase space with a grid of spacing δ . Then we perform the Monte Carlo simulation, but if there is a rejection during a trial step, this means that the initial state is in the boundary of the landscape. To look at the coordination in phase space of this state, a movement in each of the DN coordinates of the grid is performed, as in Eq. (5), but for each coordinate q_r taken in sequence from $r=1$ to $r=DN$. For each coordinate movement, the new state is tested in order to determine if its an allowed or forbidden state. After this cycle in the coordinates, the number of accepted states is the coordination number $z_k(\delta)$. The process continues until a new rejection appears, and at the end of the simulation, the average and the standard deviation of the distribution of $z_k(\delta)$ are obtained. The same procedure is repeated for different scales δ .

Figure 1 illustrates the procedure for a very simple system. Consider two disks in a box of length L and width σ . In such a case, the movement is one dimensional. If x_1 and x_2 are the coordinates of each disk, the configurational part of the phase space can be represented as a plane. The shape of the landscape is determined by the condition of nonoverlap $|x_1 - x_2| \geq \sigma$ and the walls of the box. The allowed phase space is made by two triangles, as shown in Fig. 1. Notice that ergodicity is always broken since the two triangular regions are not connected. In Fig. 1, the grid is indicated as dotted lines; the points at the boundary (open circles in Fig. 1) are those connected to grid points that are outside the triangular regions (closed circles).

In this simple system, it is very instructive to compare the rejection ratio of the Monte Carlo method with the topology of the phase space, since the theoretical value for $M_B(\delta)/M(\delta)$ for a given packing fraction $\phi = 2/L$ is easy to find. The value of $M_B(\delta)/M(\delta)$ in this case is given by the ratio between perimeter area of the triangle as a function of the scale

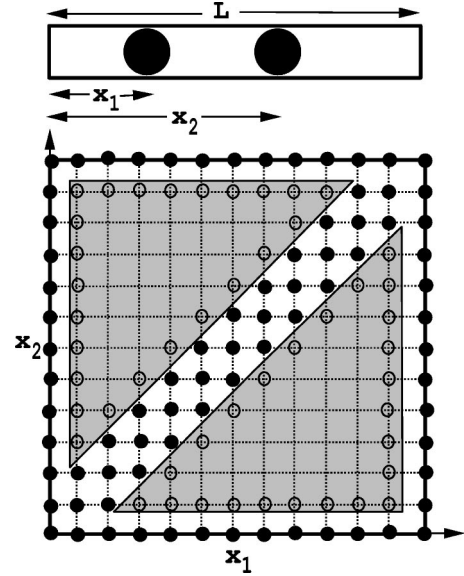


FIG. 1. Two disks in a rectangular box of length L and width σ . Below the box, the corresponding configurational part of the phase space is shown. The allowed part of the landscape is the area indicated with the grey shadow. A grid of scale δ is indicated by dotted lines. Boundary points are indicated by open circles. Closed circles are states in the forbidden part of the phase space. Notice that in this problem, ergodicity is always broken, since the allowed parts of the landscape are not connected.

$$\left[\frac{M_B(\delta)}{M(\delta)} \right]_L = \left(\frac{2(2 + \sqrt{2})}{L(1 - 2\sigma/L)} \right) \delta,$$

where the subscript is used to indicate that the result depends on the corresponding length of the box. This result can be related with the probability of rejection of the Monte Carlo simulation as follows. If we suppose an uniform sampling, the probability of hitting a boundary point is given by the perimeter-area ratio of the triangles. The average coordination of the boundary points can be obtained from a direct inspection of the drawings with different grids, that gives $\langle z(\delta) \rangle \approx \sqrt{2} + (3/2)$ for $\sigma \ll L$. We can neglect the term $\hat{\sigma}(\delta)/4$, since it is very small to be considered (this approximation was confirmed afterwards by the coordination statistics obtained from the Monte Carlo simulation). Using Eq. (11), the predicted rejection probability is

$$p^R(\delta) = m(L) \delta,$$

where $m(L)$ is defined as

$$m(L) \equiv \left(\frac{5}{8} - \frac{1}{2\sqrt{2}} \right) [M_B(\delta)/M(\delta)]_L.$$

The rejection is thus expected to be proportional to δ , as confirmed in Fig. 2 by the numerical simulations using a Monte Carlo method, where the rejections are plotted against δ for different L . Using a least-square fitting, the slopes for each of the lines is shown in Fig. 3 using a log-log plot. The solid curve is the theoretical value of $m(L)$ and the squares are the results of the simulation using the Monte Carlo simulation. These results are in very good agreement with the

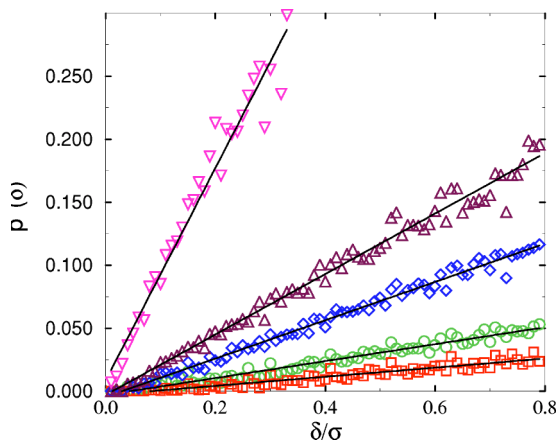


FIG. 2. Rejection ratio as a function of the scale δ (measured in units of σ) for $L=50\sigma$ (squares), 30σ (circles), 15σ (diamonds), 10σ (triangles up), and 4σ (triangles down).

theoretical values, specially for $\sigma \ll L$, where $m(L)$ is well approximated by

$$m(L) \approx \frac{8(2 + \sqrt{2})}{L} (1 + 2\sigma/L),$$

so $m(L) \sim L^{-1}$, and $D_f=1$ as expected for a smooth surface. In the region $\sigma \approx L$, the difference between both results is due to the fact that the average coordination number is not anymore $\sqrt{2}+(3/2)$, and a correction is needed in the analytical formula. Also, in this region the sampling is far from uniform, since the grid is very small compared with the size of the boundary.

III. SCALING IN A SIMPLE LIQUID

In this section, we show the results obtained using the method proposed in the previous section for a two-

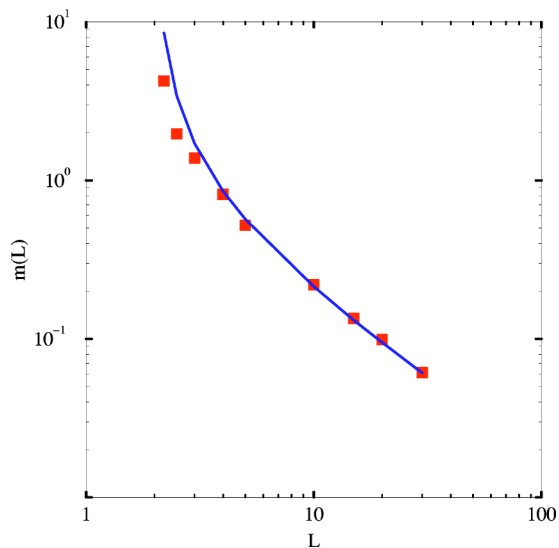


FIG. 3. Slopes of the fitting lines that appear in Fig. 2 as a function of L . The solid line is the function $m(L)$.

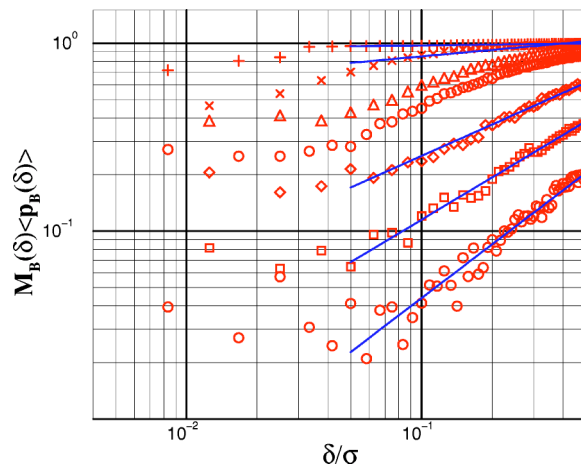


FIG. 4. Parameter $M_B(\delta)\langle p_B(\delta) \rangle$ as a function of the scale δ , for different packing fractions. From top to bottom, $\phi=0.74$ (squares), $\phi=0.71$ (\times), $\phi=0.39$ (triangles), $\phi=0.23$ (stars), $\phi=0.12$ (diamonds), $\phi=0.08$ (squares), and $\phi=0.04$ (filled circles). The lines were obtained using a power law fit.

dimensional system composed of hard-disks at different packing fractions $\phi=N\pi\sigma^2/4S$, where $N=100$ particles. The thermodynamics of this system has been investigated by many different groups during the past 50 years [40–42]. Despite the simplicity of the model, the nature of the phase transition from solid to fluid is still debated [43], as well as the nature of local order [44] and its relation with some peaks in the radial distribution function [45]. Here we will only investigate the landscape scaling. Figure 4 shows a log-log plot of $M_B(\delta)\langle p_B(\delta) \rangle$ as a function of δ for different packing fractions, as indicated in the figure caption. Figure 5 is a similar plot, but only for packing fractions near the freezing point (denoted by ϕ_0). Both plots give evidence that there is a power law scaling of $M_B(\delta)\langle p_B(\delta) \rangle$ with δ . This power law behavior is clear near the freezing point or at low densities, where fits of the type δ^{D_f} are shown for the different sets of data (only fits with correlation coefficients bigger than 99% are shown). Notice that all the fits have a cutoff at

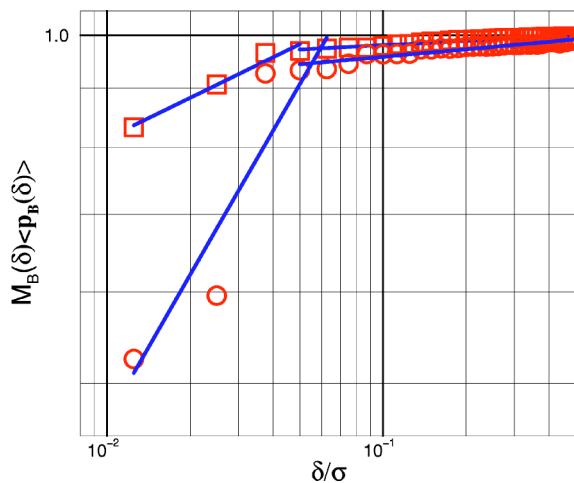


FIG. 5. Parameter $M_B(\delta)\langle p_B(\delta) \rangle$ close to freezing as a function of δ , at $\phi=0.74$ (squares) and $\phi=0.63$ (circles).

$\delta=0.05\sigma$, since there is a crossover in the power law behavior, i.e., for a given packing fraction, two regions with different scaling exponents are observed, as seen in Fig. 5, where a drop of $M_B(\delta)\langle p_B(\delta) \rangle$ is observed around $\delta=0.05\sigma$. For low packing fractions, the exponents for $\delta<0.05\sigma$ tend to be smaller than in the region $\delta>0.05\sigma$. The fact that two exponents are observed means that below a certain length scale, the landscape has a different structure. For all the different packing fractions, this behavior is nearly similar. We can speculate that this change of regimen for the scaling at a length scale is related with the different processes of relaxation that have been observed in diverse simulations [28,46,47] and experiments [16], since although a Monte Carlo simulation does not provide the real dynamic of the system, is clear that a big length scale δ in phase space corresponds to long times in the evolution of the system, as also expected from the Adam-Gibbs relation between relaxation times and configurational entropy [7]. However, this speculation needs to be investigated in more detail.

We also notice that for packing fractions $0.2<\phi/\phi_0<0.6$, it seems that using one single scaling exponent is not enough to fit the data, which is an indicative of a multifractal structure, although if we restrict the fitting for $\delta>0.2$, again a good power law fit is obtained.

In Fig. 6 we plot the scaling exponents obtained from the data of Figs. 4 and 5 as a function of the packing fraction, for the regions $(0.2\sigma<\delta)$ where a clear scaling is obtained for all the graphs. As shown in the figure, as the packing fraction reaches the freezing point, D_f goes to zero, and the landscape boundary scales nearly as the volume in phase space. This means that near the freezing point, the topology of the landscape restricts in a severe manner the available phase space. Thus Fig. 6 provides clear evidence of how the topology of the landscape is responsible for the phase transition that occurs at the freezing point, and reinforces the speculation about relaxation times, since it has been observed in experiments with colloids that freezing occurs when long time relaxation is no longer available [16].

IV. CONCLUSIONS

In this article, we have discussed some aspects of how to characterize the structure and texture of the energy landscape

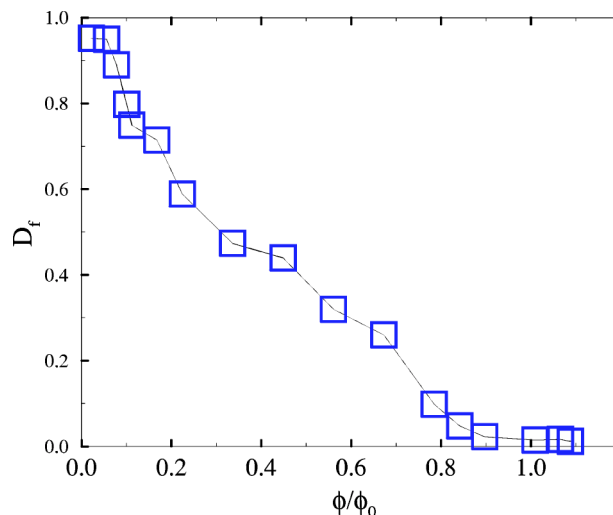


FIG. 6. Exponent D_f as a function of the ratio between the packing fraction and the packing fraction at freezing (ϕ_0). The size of the squares is proportional to the maximal error, and the line is a visual guide to the eye.

in simple fluids. As a result, we showed a method to investigate the boundary of the landscape that uses the Monte Carlo rejection ratio plus the average coordination of a state in phase space. An example of how to apply the method has been presented for a very simple model that consists of two disks that moves in one dimension. A similar procedure applied to a system of hard disks shows a clear power law scaling of the ratio between the boundary and the volume of the landscape. A crossover in the scaling exponents has been observed for a given packing fraction. Near the freezing point, the boundary of the landscape scales as the volume in phase space, and as a result the system tend to stay in pockets of the phase space. We speculate that the crossover observed in the scaling is related with the different kinds of relaxation processes of the fluid. In future works, we will further explore this idea.

ACKNOWLEDGMENTS

This work was supported by DGAPA UNAM project IN108502, and National Science Foundation-CONACyT joint project 41538.

-
- [1] D. Tabor, *Gases, Liquids and Solids* (Cambridge University Press, Cambridge, England, 1996).
 - [2] P. G. Debenedetti and F. H. Stillinger, *Nature (London)* **410**, 259 (2000).
 - [3] P. W. Anderson, *Science* **267**, 1615 (1995).
 - [4] J. C. Phillips, *Rep. Prog. Phys.* **59** 1133 (1996).
 - [5] J. Jackle, *Rep. Prog. Phys.* **49**, 171 (1986).
 - [6] M. Tatsumisago, B. L. Halfpap, J. L. Green, S. M. Lindsay, and C. A. Angell, *Phys. Rev. Lett.* **64**, 1549 (1990).
 - [7] P. G. Debenedetti, *Metastable Liquids* (Princeton University Press, Princeton, NJ, 1996).
 - [8] R. Kerner, *Physica B* **215**, 267 (1995).
 - [9] R. Kerner and G. G. Naumis, *J. Phys.: Condens. Matter* **12**, 1641 (2000).
 - [10] M. Micoulaut and G. G. Naumis, *Europhys. Lett.* **47**, 568 (1999).
 - [11] J. C. Phillips, *J. Non-Cryst. Solids* **34**, 153 (1979).
 - [12] M. F. Thorpe, *J. Non-Cryst. Solids* **57**, 355 (1983).
 - [13] H. He and M. Thorpe, *Phys. Rev. Lett.* **54**, 2107 (1985).
 - [14] A. Huerta and G. G. Naumis, *Phys. Rev. Lett.* **90**, 145701 (2003).
 - [15] A. Huerta, G. G. Naumis, D. T. Wasan, D. Henderson, and A. Trokhymchuk, *J. Chem. Phys.* **120**, 1506 (2004).
 - [16] E. R. Weeks, J. C. Crocker, A. C. Levitt, A. Schofield, and D.

- A. Weits, *Science* **287**, 627 (2000).
- [17] M. Goldstein, *J. Chem. Phys.* **64**, 11 (1976).
- [18] A. Angell, *Nature (London)* **393**, 521 (1998).
- [19] M. Mézard and G. Parisi, *Spin Glass Theory and Beyond* (World Scientific, Singapore, 1987).
- [20] F. H. Stillinger, *Phys. Rev. E* **59**, 48 (1999).
- [21] S. Büchner and A. Heuer, *Phys. Rev. E* **60**, 6507 (1999).
- [22] P. Shah and Ch. Chakravarty, *Phys. Rev. Lett.* **88**, 255501 (2002).
- [23] M. Scott Shell and P. G. Debenedetti, *Phys. Rev. E* **69**, 051102 (2004).
- [24] G. G. Naumis, *Phys. Rev. B* **61**, R9205 (2000).
- [25] J. P. K. Doye, *Phys. Rev. Lett.* **88**, 238701 (2002).
- [26] T. Keyes and J. Chowdhary, *Phys. Rev. E* **65**, 041106 (2002).
- [27] Y. V. Fyodorov, *Phys. Rev. Lett.* **92**, 240601 (2004).
- [28] T. Keyes, *Phys. Rev. E* **59**, 3207 (1999).
- [29] A. Van Blaaderen, *Science* **301**, 471 (2003).
- [30] V. N. Marcharan, M. T. Elsesser, and D. J. Pines, *Science* **301**, 483 (2003).
- [31] T. L. Saaty and J. Bram, *Nonlinear Mathematics* (Dover Books, New York, 1964).
- [32] D. S. Cort, P. G. Debenedetti, S. Sastry, and F. H. Stillinger, *Phys. Rev. E* **55**, 5522 (1997).
- [33] K. Falconer, *Fractal Geometry* (John Wiley & Sons, New York, 1997).
- [34] G. Ciccotti, D. Frenkel, and I. R. McDonald, *Simulations of Liquids and Solids* (North-Holland, Amsterdam, 1987).
- [35] K. Binder and D. W. Heermann, *Monte Carlo Simulation in Statistical Physics*, 3rd ed. (Springer-Verlag, Berlin, 1977).
- [36] M. P. Allen and D. J. Tildesley, *Computer Simulation of Liquids* (Oxford Science Publications, Oxford, 2003).
- [37] S. Jain, *Monte Carlo Simulation of Disordered Solids* (World Scientific, Singapore, 1991).
- [38] B. D. Lubachevsky and F. H. Stillinger, *J. Stat. Phys.* **60**, 561 (1990).
- [39] G. G. Naumis, Ch. Wang, and R. Barrio, *Phys. Rev. B* **65**, 134203 (2002).
- [40] N. Metropolis, A. W. Rosenbluth, M. N. Rosenbluth, and A. H. Teller, *J. Chem. Phys.* **21**, 1087 (1953).
- [41] B. J. Alder and T. E. Wainwright, *J. Chem. Phys.* **33**, 1439 (1960).
- [42] W. G. Hoover and B. J. Alder, *J. Chem. Phys.* **46**, 686 (1967).
- [43] S. Sengupta, P. Nielaba, and K. Binder, *Phys. Rev. E* **61**, 6294 (2000).
- [44] F. H. Stillinger, D. K. Stillinger, S. Torquato, T. M. Truskett, and Pablo G. Debenedetti, *J. Chem. Phys.* **113**, 10186 (2000).
- [45] T. M. Truskett, S. Torquato, S. Sastry, P. G. Debenedetti, and F. H. Stillinger, *Phys. Rev. E* **58**, 3083 (1998).
- [46] R. J. Speedy, *Mol. Phys.* **62**, 509 (1987).
- [47] J. J. Erpenbeck and W. W. Wood, *Phys. Rev. A* **43**, 4254 (1991).